Rev. Adv. Mater. Sci. 31 (2012) 12-18

THE ROLE OF FRICTION IN TUBULAR CHANNEL ANGULAR PRESSING

Ghader Faraji[1], Mahmoud Mosavi Mashhadi[1], Soo-Hyun Joo[2] and Hyoung Seop Kim[2]

[1]Department of Mechanical Engineering, University College of Engineering, University of Tehran, Tehran, 11155-4563, Iran
[2]Department of Materials science and Engineering, POSTECH, Pohang, 790-784, Korea

Received: April 20, 2012

Abstract. In this paper, numerical, analytical, and experimental investigations were undertaken in order to clarify the influence of friction in tubular channel angular pressing (TCAP) as a severe plastic deformation technique for producing nanostructured pipes. The effects of different Coulomb friction coefficients of 0, 0.025, 0.05, 0.075, and 0.1 on the deformation behavior and required load were investigated using the finite element method (FEM). The results showed that the friction coefficient in the TCAP has a significant effect on the required load due to the variation in the friction force during the TCAP. A comparison between the FEM and experimental results showed that the Coulomb friction coefficient is approximately 0.055 in the TCAP process when MoS_2 was used as a lubricant. The analytical investigation results in the calculation of the equivalent plastic strain were close to those of the FEM when the friction coefficient increased from 0 to 0.1. The die corner gap in shear zone III decreased with the increasing friction coefficient.

1. INTRODUCTION

There has been much interest in recent years in improving material properties by severe plastic deformation (SPD). There are many SPD methods for producing ultrafine grained (UFG) and nanostructured bulk and sheet materials with superior mechanical properties [1-6], such as equal channel angular pressing (ECAP) [2,4,5], twist extrusion (TE) [7], ECAP-conform [8], simple shear extrusion (SSE) [9], accumulative back extrusion (ABE) [10,11] for bars, accumulative roll bonding (ARB) [12], continuous confined strip shearing (C2S2) [13], groove pressing (GP) [14] for sheets, high pressure torsion (HPT) [3,6,15] for disks. Beside the numerous processes for bulk and sheet materials, some SPD methods have been developed recently that can produce UFG pipes such as high-pressure tube twisting (HPTT) developed by Toth *et al*. [16] and accumulative spin bonding (ASB) developed by Mohebbi and Akbarzadeh [17]. Recently an effective process based on ECAP named the tubular channel angular pressing (TCAP), which is suitable for processing tubes at high strains, was proposed by Faraji *et al*. [18]. A schematic of the TCAP is shown in Fig. 1. The constrained tube between the inner and outer dies is pressed by a hollow cylindrical punch into a tubular angular channel. The tube material is pressed into the tubular angular channel where three shear events occur in three forming zones (I, II, and III) during one processing cycle. Three channel angles (φ_1, φ_2, and φ_3) and three corner angles (ψ_1, ψ_2, and ψ_3) determine the total strain, which is the main factor controlling the microstructural evolution. Because the TCAP process is a new technique, there are many unknown variables that affect the processing and properties of the processed material. In par-

Corresponding author: H.S. Kim, e-mail: hskim@postech.edu and http://hskim.postech.ac.kr

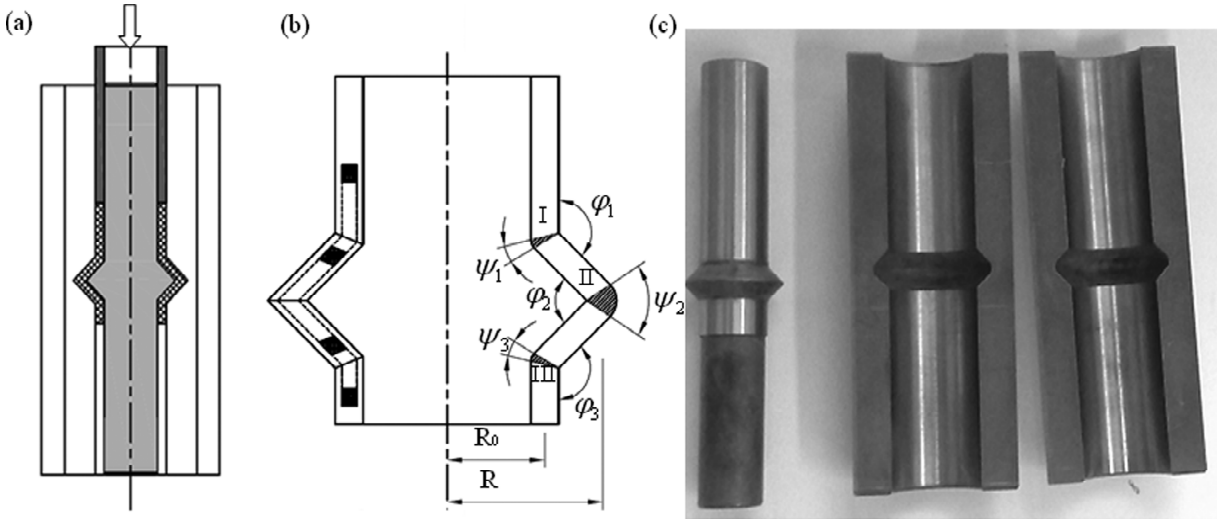

Fig. 1. (a) Schematic of the TCAP, (b) process parameters, and (c) images of the inner and outer dies.

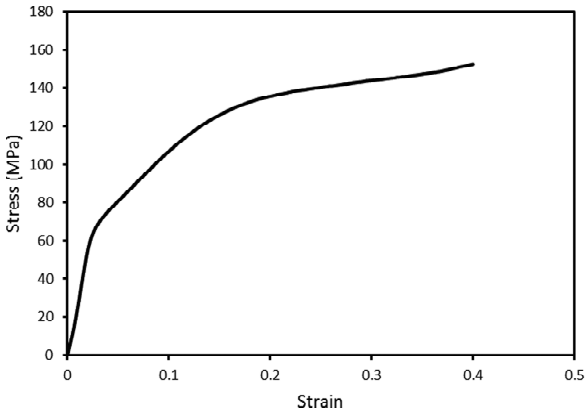

Fig. 2. Stress-strain curve of AZ91 at 300 °C.

Table 1. Physical and mechanical properties of the AZ91 experimental alloy and process parameters.

Parameter	Value
Poisson's ration	0.35
Young's modulus	41 GPa
Density	1.78 g/cm^3
Friction coefficient	0, 0.025, 0.05, 0.075, and 0.1
φ_2	90°
$\psi_1 = \psi_3$	0°
ψ_2	90°

ticular, the effect of friction on the TCAP processing needs to be elucidated due to its critical importance in metal forming.

In the present paper, the effects of friction on the deformation behavior and required load are investigated using FEM and experimental approaches. An analytical modeling was also used for a fast solution to the developed plastic strain.

2. FEM AND EXPERIMENTAL PROCEDURES

A commercial FEM code (Abaqus/Explicit) was used to perform the numerical simulations. An axisymmetric model was employed, where the geometrical dimensions and mechanical properties of the specimens were identical to those of the experiment, enabling the comparison of the simulation results with the experimental ones. Axisymmetric four node elements (CAX4R) were used to model the workpiece and dies. In order to accommodate the predetermined large strains during the simulations, adaptive meshing (automatic remeshing) was employed. The arbitrary Lagrangian–Eulerian (ALE) adaptive meshing maintains a high-quality mesh under SPD by allowing the mesh to move independently with respect to the underlying material. The Coulomb friction and penalty method were used to model the contact conditions between the die and the specimen. The die and the punch were modeled as analytical rigid parts. The friction coefficients of 0, 0.025, 0.05, 0.075, and 0.1 were considered. The mechanical properties of the AZ91 alloy shown in Fig. 2 were obtained through a compression test at the TCAP processing temperature of 300 °C under a strain rate of 1x10^{-3} sec^{-1}. The experimental alloy properties and process parameters are shown in Table 1.

The material used in this study was a commercial AZ91 magnesium alloy. Cylindrical tubes of 20 mm in outer diameter, 2.5 mm in thickness, and 35 mm in length were machined from cast ingots. A TCAP die was manufactured from hot worked tool steel and hardened to 55 HRC. The channel angles

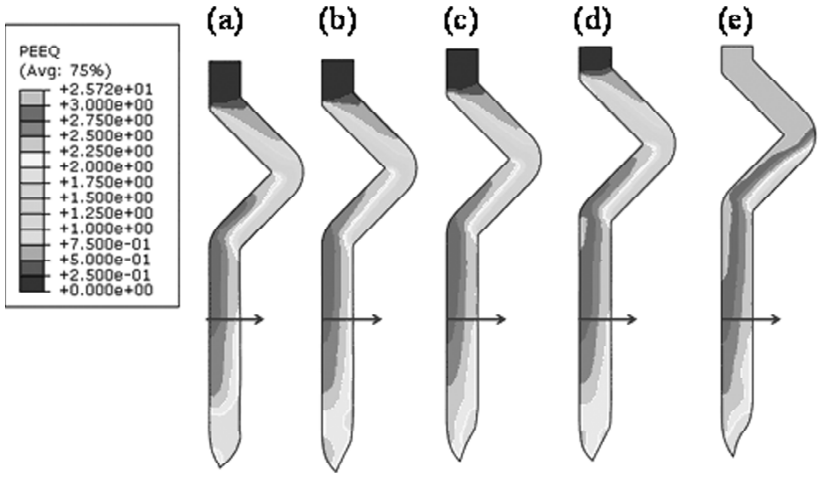

Fig. 3. Equivalent plastic strain contours of the TCAP processed tube with different friction coefficients: (a) 0, (b) 0.025, (c) 0.05, (d) 0.075, and (e) 0.1.

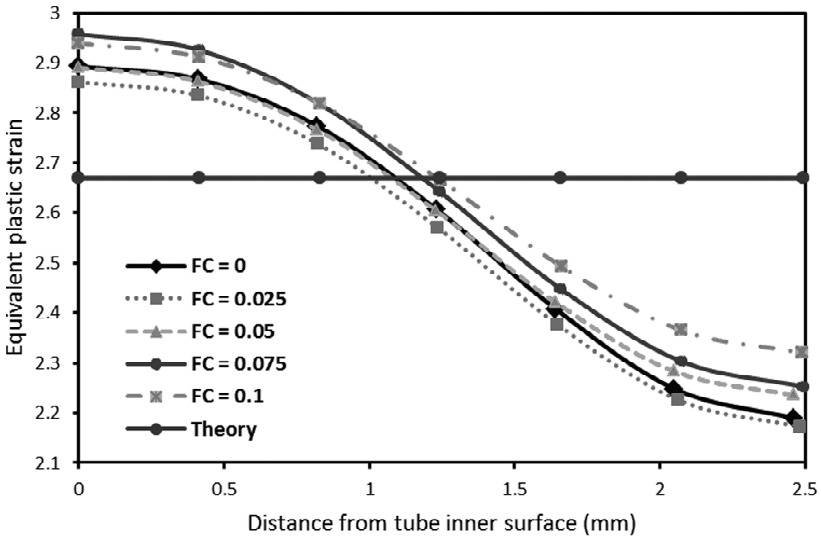

Fig. 4. Equivalent plastic strain versus distance from the inner surface of the processed tube.

φ_1, φ_2, and φ_3 in the TCAP facility were 135°, 90°, and 135°, respectively. The angle of curvature ψ_2 was 90°, and both ψ_1 and ψ_3 were equal to 0°, as in Fig. 1. The specimens were subjected to TCAP at 300 °C with a punch speed of 5 mm/min to minimize increases in the temperature during the deformation. The temperature increase was observed to be less than 5 °C at a pressing speed of 11 mm/min [19]. The friction between the specimen and dies was reduced by applying MoS_2 as a lubricant.

3. RESULTS AND DISCUSSION

The equivalent plastic strain achieved during the deformation is shown in Fig. 3. In all frictional cases, the equivalent plastic strain in the TCAP processed tube was smaller along the outer surface than in the other regions, while it was high in the inner surface in the cases with friction coefficients from 0 to 0.075. It can also be seen that the strain values after shear zone II for the friction coefficient of 0.075 were higher than the other cases. Fig. 3e shows that the friction coefficient of 0.1 caused the highest strain value in the tail region. The high strain in this region is due to the high back pressure effect under high friction, which is explained in the following session.

Fig. 4 shows the predicted equivalent plastic strain through the tube thickness shown by the arrows in Fig. 3. The theoretical equivalent plastic strain calculated from the constitutive equations of the TCAP proposed by Faraji *et al*. [18] is also presented in Fig. 4, showing a single uniform value across the tube thickness. The theoretical equations did not consider the influences of the material behavior and friction. Hence, the theoretical equivalent plastic strain is a straight line with a value of approximately 2.69. The FEM simulated equivalent

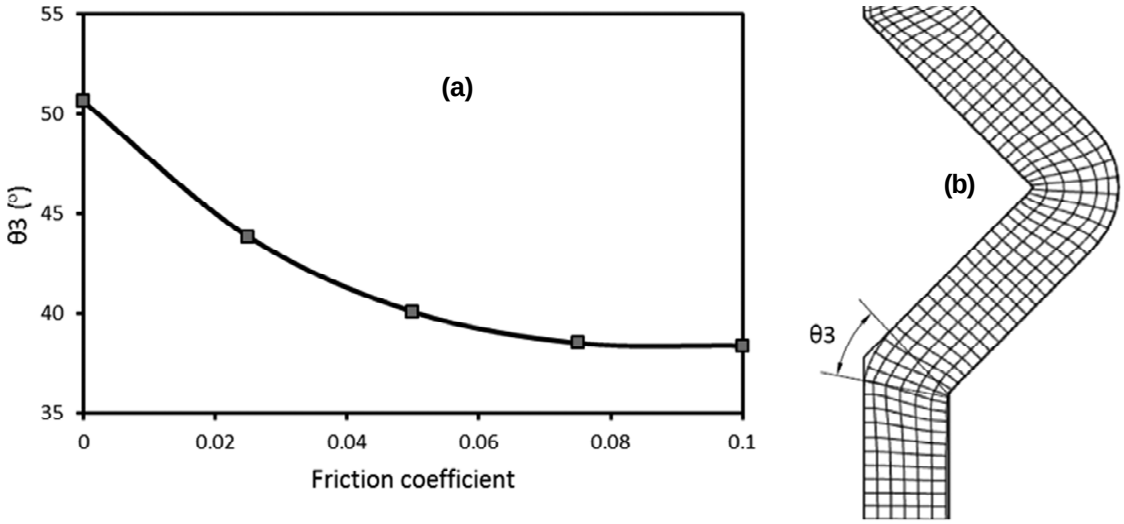

Fig. 5. Effect of friction coefficient on the gap region between the inner die and processed tube.

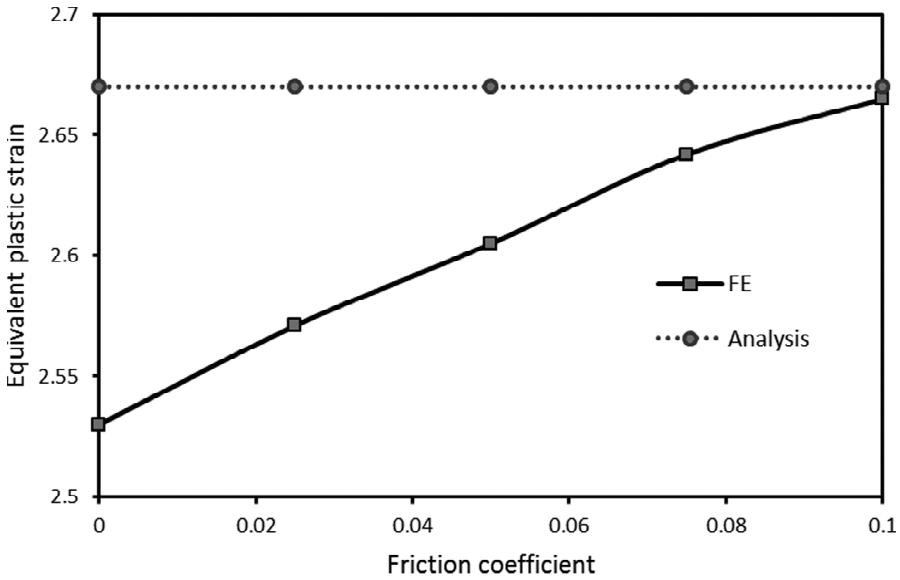

Fig. 6. Equivalent plastic strain value versus friction coefficient (the FEM value is the mean of the strain value through the tube thickness).

plastic strain curves have the same trend in different friction coefficients: decreased strain with the position from the inside to the outside. It should be noted that the different friction coefficients derived different trends in equivalent plastic strain curves in the conventional ECAP which was noted by Nagasekhar *et al*., [20]. The maximum equivalent plastic strain occurs in the inner surface of the tube and the minimum occurs in the outer surface of the tube. In the outer surface, the equivalent plastic strain value is increased by increasing the friction coefficient. Also, it can be seen that the mean value of the FEM results is almost identical to the theoretical value. Thus, there is a reasonably good agreement between the average strain of the FEM and the theoretical analysis.

Kim *et al*. [21] mentioned that a corner gap between the die and the workpiece is usually found during the ECAP of strain hardening materials. Similarly, the real corner angle of the workpiece is an arc curvature of the workpiece θ_3 as shown in Fig. 5b, not the die corner angle ψ_3 due to the corner gap formation. If the die is fully filled by the processed material, the angles of θ_3 and ψ_3 will be identical. The corner gap rarely occurs in forming zone I due to the high back pressure that results from forming zones II and III. In forming zone III where the back pressure is negligible, the corner angle of the workpiece (θ_3) is higher than the die corner angle ψ_3.

Fig. 5a shows the effect of the friction coefficient on the θ_3 value. It can be seen clearly that θ_3 de-

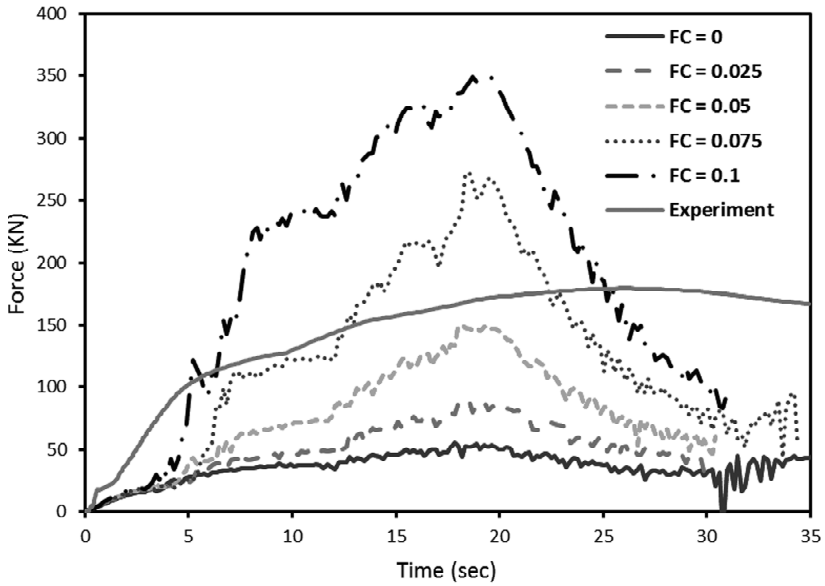

Fig. 7. FEM calculated pressing load versus ram displacement during TCAP processing with friction coefficients of 0, 0.025, 0.05, 0.075, and 0.1.

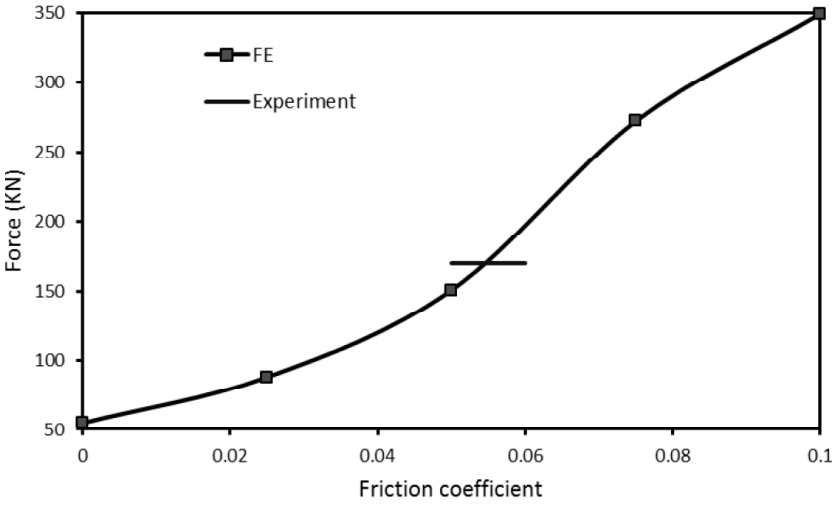

Fig. 8. Peak load calculated for the TCAP of AZ91 from the FEM for different friction coefficients and the experiment.

creases with the friction coefficient, which is the same as Yoon *et al*. [22] results in the conventional ECAP. Kim *et al*. [23] mentioned that in the conventional ECAP, the die corner gap causes a decrease in the equivalent plastic strain as a result of the increase in the θ_3 (actual curvature angle on workpiece). While the analytical calculation is based on the die corner angle ψ, the FEM calculations are based on the actual corner angle of the workpiece θ; there is a difference between the FEE (mean value through tube thickness) and the theoretical analysis, as seen in Fig. 6. It should be noted that the difference decreases with increases in the friction coefficient, due to the increase in the friction coefficient leading to a small corner gap and consequently the workpiece geometry develops into the same as that if the die geometry.

Fig. 7 shows the calculated load plotted against the ram displacement curves for the TCAP with various friction coefficients. The processing load increases with the friction coefficient due to the additional energy spent in recovering the deformation resistance in the surface [24]. There are three slope regions in all cases, corresponding to the three forming zones. The slope decreases with a decreasing friction coefficient. An important feature in the force curves is that all curves tend to converge, which may be attributed to the friction force. Considering the Coulomb friction type, the friction force is the friction coefficient multiplied by the normal force.

During the TCAP, if the tube is divided into two sections axially, before and after the last forming zone III, the hydrostatic pressure in the regions before forming zone III is higher, while it decreases zero in the region after forming zone III. That is, the normal force in the region before forming zone III is high, while in the region after forming zone III it approaches zero. During the processing, the tube region before forming zone III decreases and the tube region after forming zone III increases. That is, the friction force decreases gradually. Therefore, the total force curve decreases after the tube passes forming zone III in all friction coefficients. Because the ratio of the friction force to the total force is higher under higher friction coefficients, the force decrement in the higher friction coefficients is higher than the smaller decrements.

The influence of the friction coefficient on the peak load required in the TCAP is shown in Fig. 8. With increases in the friction coefficient, the peak load required to pass the tube from shear zone III is increased. Also, the peak loads corresponding to every shear zone are increased. From this figure, when the friction coefficient is between 0.05 and 0.06, the peak load calculated from the FEM results is similar to the experimental peak load. Hence, the friction coefficient can be estimated to be approximately 0.055 in the TCAP when the MoS_2 lubricant is used [25,26].

4. CONCLUSIONS

The influence of the friction coefficient in TCAP processing was investigated using FEM analyses and experimental approaches. Five different friction coefficients of 0, 0.025, 0.05, 0.075, and 0.1 were employed. The results demonstrates that the friction coefficient had a significant effect on the required load in the TCAP and the required loads for different friction coefficients converge to the force for the frictionless case due to the variation of the frictional force during the TCAP. Comparisons between the FEM analyses and the experimental results demonstrated that the friction coefficient was estimated to approximately 0.055 in the TCAP when the MoS_2 lubricant is used. The analytical solution results in the equivalent plastic strain are close to the FEM results when the friction coefficient is increased from 0 to 0.1. The die corner gap in forming zone I is almost zero as a result of the back pressure, while it increases in forming zone III and decreases with an increasing friction coefficient.

ACKNOWLEDGEMENTS

The authors would like to acknowledge the partial financial support of the University of Tehran. HSK acknowledges the support by a grant from the Fundamental R&D Program for Core Technology of Materials (10037206) funded by the Ministry of Knowledge Economy, Republic of Korea.

REFERENCES

[1] R.Z. Valiev, R.K. Islamgaliev and I.V. Alexandrov // *Prog. Mater. Sci.* **45** (2000) 103.
[2] R.Z. Valiev and T.G. Langdon // *Prog. Mater. Sci.* **51** (2006) 881.
[3] A.P. Zhilyaev and T.G. Langdon // *Prog. Mater. Sci.* **53** (2008) 893.
[4] M.I.A.E. Aal, N.E. Mahallawy, F.A. Shehata, M.A.E. Hameed, E.Y. Yoon, J.H. Lee and H.S. Kim // *Metal. Mater. Inter.* **16** (2010) 709.
[5] M. Vaseghi, A. K. Taheri and H. S. Kim // *Metal. Mater. Inter.* **16** (2010) 363.
[6] Y. Song, E.Y. Yoon, D.J. Lee, J.W. Lee and H.S. Kim // *Mater. Sci. Eng. A* **528** (2011) 4840.
[7] Y. Beygelzimer, A. Reshetov, S. Synkov, O. Prokofeva and R. Kulagin // *J. Mater. Proc. Tech.* **209** (2009) 3650.
[8] G.J. Raab, R.Z. Valiev, T.C. Lowe and Y.T. Zhu // *Mater. Sci. Eng. A* **382** (2004) 30.
[9] N. Pardis and R. Ebrahimi // *Mater. Sci. Eng. A* **527** (2009) 355.
[10] G. Faraji, M.M. Mashhadi and H.S. Kim // *Mater. Sci. Eng. A* **528** (2011) 4312.
[11] G. Faraji, M.M. Mashhadi and H.S. Kim // *Mater. Manuf. Proc.* **27** (2012) 267.
[12] Y. Saito, N. Tsuji, H. Utsunomiya, T. Sakai and R.G. Hong // *Scripta Mater.* **39** (1998) 1221.
[13] J.C. Lee, H.K. Seok and J.Y. Suh // *Acta Mater.* **50** (2002) 4005.
[14] S.C. Yoon, A. Krishnaiah, U. Chakkingal and H.S. Kim // *Compu. Mater. Sci.* **43** (2008) 641.
[15] H.S. Kim // *J. Mater. Proc. Tech.* **113** (2001) 617.
[16] L.S. Toth, M. Arzaghi, J.J. Fundenberger, B. Beausir, O. Bouaziz and R. Arruffat-Massion // *Scripta Mater.* **60** (2009) 175.
[17] M.S. Mohebbi and A. Akbarzadeh // *Mater. Sci. Eng. A* **528** (2010) 180.
[18] G. Faraji, M.M. Mashhadi and H.S. Kim // *Mater. Lett.* **65** (2011) 3009.
[19] H.S. Kim // *Mater. Trans.* **42** (2001) 536.

[20] A.V. Nagasekhar, S.C. Yoon, Y. Tick-Hon and H.S. Kim // *Compu. Mater. Sci.* **46** (2009) 347.
[21] H.S. Kim, M.H. Seo and S.I. Hong // *J. Mater. Proc. Tech.* **113** (2001) 622.
[22] S.C. Yoon, A. Krishnaiah, U. Chakkingal and H.S. Kim // *Compu. Mater. Sci.* **43** (2008) 641.
[23] H.S. Kim, M.H. Seo and S.I. Hong // *Mater. Sci. Eng. A* **291** (2000) 86.
[24] G. Purcek, O. Saray and O. Kul // *Metal. Mater. Inter.* **16** (2010) 145.
[25] J.H. Noh, J.M. Seo and B.B. Hwang // *Metal. Mater. Inter.* **17** (2011) 187.
[26] J.Y. Im, J.H. Noh and B.B. Hwang // *Trans. Mater. Proc.* **19** (2010) 494.